C. elegans Inositol 5- Phosphatase Homologue Negatively Regulates Inositol 1,4,5-triphosphate Signaling in Ovulation

Yen Kim Bui and Paul W. Sternberg[1]
Howard Hughes Medical Institute and Division of Biology, California Institute of Technology, Pasadena, CA, 91125 USA

[1] Correspondence should be addressed to PWS
Phone 626-395-2181
Fax 626-569-8012
pws@caltech.edu

Key words: Epidermal growth factor signaling, inositol triphosphate kinase, inositol 5-phosphatase, rhythmic behavior

Abstract

Ovulation in *Caenorhabditis elegans* requires IP_3 signaling activated by the EGF-receptor homolog LET-23. We generated a deletion mutant of a type I 5-phosphatase, *ipp-5,* and find a novel ovulation phenotype whereby the spermatheca hyperextends to engulf two oocytes per ovulation cycle. The temporal and spatial expression of IPP-5 is consistent with its proposed inhibition of IP_3 signaling in the adult spermatheca. *ipp-5* acts downstream of *let-23,* and interacts with *let-23*-mediated IP_3 signaling pathway genes. We infer that IPP-5 negatively regulates IP_3 signaling to ensure proper spermathecal contraction.

INTRODUCTION

A crucial aspect of signal transduction is understanding how regulatory mechanisms ensure a precise biological response to pathway activation. Activation of receptor tyrosine kinases (RTK) stimulates phospholipase C to hydrolyze phosphatidyl 4,5-bisphosphate (PtdIns[4,5]P_2) to inositol 1,4,5 triphosphate (IP_3), which binds the tetrameric IP_3 receptor to mobilize intracellular calcium (Majerus,1992; Berridge,1993). IP_3 signaling mediates many cellular processes (Berridge and Irvine, 1989; Berridge,1993; Figure 1). Mechanisms for attenuating and terminating signaling, such as provided by proteins that metabolize IP_3, are critical to maintain fine control of the physiological responses dependent on IP_3 mediated calcium release. It is thus important to understand negative regulation of IP_3 signaling.

Previous biochemical studies have shown how IP_3 is produced (Berridge and Irvine, 1984), how it is metabolized (Majerus,1992), and how it releases intracellular calcium (Berridge, 1995; Bootman and Berridge, 1995; Clapham, 1995); however they have not directly addressed IP_3 function in an intact metazoan. Two enzymes have been biochemically identified that participate in IP_3 metabolism and potentially regulate signaling output: inositol 1,4,5 triphosphate kinase (IP_3K) and inositol polyphosphatase 5-phosphatase (Majerus, 1992; Drayer et al., 1996). 5-phosphatases lower IP_3 levels by dephosphorylating the 5' phosphate and vary in substrate specificity (Mitchell et al., 1996; Erneux et al., 1998). Type I 5-phosphatases are the most active in hydrolyzing IP_3 and IP_4, (Verjans et al., 1992; Laxminaryayan et al., 1993). Thus, they likely play a larger role in regulating cellular levels of IP_3 than do the type II phosphatases, which additionally hydrolyze the 5'-phosphoinositols, PtdIns(4,5)P_2 and PtIns(3,4,5) P_3 (Mitchell et al., 1996). The distinct functional roles of various type II 5-phosphatase family members have been demonstrated by examining targeted deletions of mammalian type II 5-phosphatases in mice (Helgason et al., 1998; Janne et al., 1998; Cremona et al., 1999) and targeted disruption of type II 5-phosphatases in yeast (Stolz et al., 1996). The functional consequence of removing type I 5-phosphatase activity *in vivo* is unknown.

Ovulation in *C. elegans* hermaphrodites provides a genetic system to study regulation of IP_3 signaling *in vivo*. *C. elegans* mutants defective in IP_3K, *lfe-2,* have no obvious ovulation defect, suggesting that an alternate pathway to metabolize IP_3 and inhibit signaling exists in *C. elegans.* Here, we report the characterization of the gene, *ipp-5,* that encodes the *C. elegans* type I 5-phosphatase. We demonstrate it acts downstream of the LET-23 RTK, based on epistasis analyses. We present for the first time, *in vivo* characterization of a type I 5-phosphatase in an intact animal by describing ovulation defects of a deletion mutant *ipp-5(sy605)* in *C. elegans* and place the negative regulatory function of a type I 5-phosphatase in a behavioral context.

MATERIAL AND METHODS

Genetic Strains

Standard methods for maintaining *C. elegans* at 20°C were used. EMS (50 mM) was used as a mutagen (Brenner, 1974). Bristol strain N2 was used as the wild type. The following alleles were used: LG1, *unc-57(ad592), lfe-2(sy326)*; LGII, *unc-4(e120), let-23(sy10), let-23(sa62)*; LGIV, *unc24(e138), lin-3(n1058), lfe-1/itr-1(sy290), dec-4(sa73)*; LGX, *lon-2(e678), unc-6(e78), ipp-5(sy605). szT1[lon-2(e678)]* is a reciprocal I;X translocation balancer. *mnC1[dpy-10(e128) unc-52(e444)]* is a rearrangement balancer chromosome on LGII. *DnT1[nT1[unc(n745dm)let]* is a reciprocal IV;V

translocation balancer. (Strains are from Brenner 1974; Ferguson et al, 1985; Fodor, A., and Deak, P., 1985; Aroian et al., 1991; Iwasaki et al., 1995; Katz et al., 1996; Clandinin et al., 1998).

Brood Assay
L4 larvae hermaphrodites were serially transferred to fresh plates every 12 hrs for 4 days at 20°C and progeny counted two days after eggs hatched.

PCR
A PCR based strategy was used to screen a library of 245,000 EMS mutagenized N2 haploid genomes for a targeted deletion in *ipp-5* (using the method of G. Moulder and R. Barstead, personal comm. http://pcmc41.ouhsc.edu/Knockout/). The deletion removes 242 bp upstream of the ATG through 25 bp of exon 3. The following primers were used to detect the deletion in lysates: Round I, JC43 (5' TGCCTTGCACAAGATTATCG) and JC46 (5' CTCTCCTTCTTCCACCAA); Round II, JC30 (5'CAGCCCATGAGTCACTACTTCC) and JC68 (5' CTAGGAGGTTTTGAATTTTGACCTG). Wild-type animals amplify a 1300 bp product while *ipp-5* deletion mutants amplify a 480 bp product. The deletion mutant was backcrossed seven times to *lon-2 unc-6*. The presence of the deletion in double mutants was verified by PCR using primer pairs JC68 and BY4 (5' CGTTTTCCTTTGACGAAAGCTCGG) in Round II to distinguish homozygotes (700 bp band) from heterozygotes (700 bp, 1600 bp band). The mutants were scored by Nomarski video recordings of ovulation.

Microscopy and image processing
Worms were anesthetized for 30 min in a solution of M9 with 0.1% tricaine and 0.01% tetramisole (Sigma Inc.) before recording (McCarter et al., 1999). Animals were mounted on 5% agarose pads with 20 µl of anesthetic, covered with an 18 mm glass cover slip, and the edges of the cover slip were sealed with Vaseline. Observations were made at 20°-23° C. Animals were mounted on a Zeiss Axioscope and recorded under Nomarski optics (Plan 100X objective) for no more than 4 hours. The microscope was connected to a MTI 72 CCD video camera module and VCR. Images were recorded on VHS tape in real time. While under anesthetic, oocyte maturation, sheath and spermathecal activity at ovulation proceed while pharyngeal pumping and egg laying cease (McCarter et al., 1999). Spermathecal extension distance was calculated by direct measurement of length (starting from the side of the proximal oocyte nearest the spermatheca to the point at which the spermathecal valve closes to envelop the oocytes) on the monitor during video production. Distance was calibrated on each set up to convert cm on the monitor to true µm values using a stage micrometer. For ovulation movies, VHS video recordings were dubbed onto DVCAM digital tapes, captured as computer DV stream files via fire wire, and then the frame speed increased by 900% using the software program Final Cut Pro. Video compression for web playback was performed using the Cleaner 5 Software Application. Still frame images (720X480 pixels) were grabbed from the ovulation computer captured DV stream file (Digital Media Center, Caltech).

For fluorescent microscopy, animals were viewed with 100X objective under a GFP filter. Images were collected using a Hamamatsu C4742-95 digital camera,

transferred to a G3 Macintosh running Open Lab Imaging 1.7.8r3 Software, and assembled in Photoshop.

***ipp-5* cDNA sequence analysis**

A full length cDNA, yk341d7, kindly provided by Yuji Kohara (EST partial sequence GenBank Accession C44206), was sequenced on both strands and compared to the wild type *ipp-5* genomic sequence from the Sequencing Consortium (The *C. elegans* Sequencing Consortium, 1998) to obtain the splicing pattern. Genefinder predicts a slightly different cDNA (WormBase WS51) than the full length cDNA we sequenced (GenBank Accession AF411588). One base pair was found missing in exon 2 in the cDNA clone yk341d7, creating a frameshift premature stop codon. Genomic DNA amplified from N2 worms was sequenced on both strands and matches the sequence provided by the Consortium, indicating the mutation in the cDNA was an artifact. The mutation was repaired using Stratagene's QuikChange Site-Directed Mutagenesis Kit, yielding mut2IP5. Sequencing confirmed the mutation was corrected and that no other artifactual mutations occurred in the cDNA.

Construction of transgenes

Standard molecular biology techniques were used (Sambrook et al., 1989). To examine the *ipp-5* expression pattern, 2 kb sequence upstream of the ATG including exon 1 was amplified from genomic N2 DNA (using high fidelity LA Takara Taq) and cloned into the pGEM TA cloning vector and then subcloned into the GFP expression vector pPD95.77 (A. Fire) with MluNI and Kpn sites, yielding pYB10. The entire *ipp-5* locus was amplified from N2 genomic DNA and subcloned into pPD49.83 (A. Fire) at the Kpn/EcoRV site yielding pYB8. The entire *ipp-5* genomic region was sequenced and no extraneous mutations were found. A 2 kb sequence upstream of the start ATG codon was subcloned in place of the HS promoter at the MluNI and Kpn sites of pYB8 yielding pYB11, in order to test if the native promoter driving expression of the genomic *ipp-5* locus rescues the *sy605* phenotype.

Three constructs using heterologous promoters driving the *ipp-5* cDNA were generated. A 1.0 kb region upstream of ZK370.3 was amplified from pCeh (kindly provided by Alex Parker) using primers, SphpCeh (5' CCCGCATGCCTGCAGTTCTCCTCTCTG CC) and KpnpCeh (5' CCCCGGTACCAAAAAAATTAATTTTTTTGGGGGC) and cloned into pPD49.83 (A. Fire) at the MluN and Kpn site. A BamH1/Asp718 fragment containing the pCeh promoter was then subcloned into vector mut2IP5 with BamH1 and EcoRI/blunted sites, yielding pYB13. The promoter was sequenced to verify that no additional mutations occurred during amplification. We examined *dpy-5(e905) hIs29[pCeh361; pCeh363]*, (kindly provided by A. Parker) which carries the pCeh::GFP transgene and confirmed that the pCeh promoter shows expression in the adult spermatheca and not the sheath (A. Parker, personal comm). For pYB14, the entire cDNA from mut2IP5 was subcloned into the heat shock vector pPD49.83 (A. Fire) at the Nhe/Kpn site. For pYB15, a 3 kb *nlp-8* promoter (Nathoo, A.N. et al. 2001), which expresses in the sheath (Anne Hart, personal comm.), was amplified using primers AN46 (5' GAAGCTTCTGACTCATGTCGC) and BamH1AN49 (5' CCGCGGATCCTGCATGCATTACTGTATTCAAAATTACGGTG) from genomic DNA and subcloned into mut2IP5 using BamH1 and EcoRI/blunted sites. We examined the strain *him-5; lin-15(n795) rtEx22[nlp-8::GFP, lin-15(+)]* (kindly

provided by A. Hart) and confirmed expression in the proximal sheath cells and not in the spermatheca (A. Hart, personal comm).

Construction of transgenic strains

Transgenic strains were generated as described by Mello et al. (1991). To assess whether the genomic *ipp-5* locus including 2 kb 5' sequence upstream of the ATG rescues the phenotype in *sy605* animals, we injected pYB11 along with *myo-2::gfp* as a transformation marker. Rescue of *ipp-5(sy605)* was determined by scoring the ovulation phenotype of three lines under Nomarski optics and recording ovulations of transgenic *ipp-5(sy605) syEx[pYB11; myo-2::gfp]* worms. We observed one ovulation event in each gonad arm per animal. Moreover, *sy605* transgenics containing the heat shock transgene, pYB14 and *myo-2::gfp* also showed rescue upon induction with a heat shock pulse of 33°for 40 min in the young adult stage. The cosmids encompassing *ipp-5* did not show the expected restriction pattern, and thus were not used to assay for rescue. We built the transgenic strain *sy605 syEx[*pYB13*; myo-2::gfp]* to test rescue with a heterologous spermathecal promoter. Additionally we built the transgenic strain *sy605 syEx[pYB15; myo-2::gfp]* to test rescue with a heterologous sheath promoter. The *ipp-5::GFP* fusion was injected with pRF4 [*rol-6(su1006)*] as a transformation marker in *sy605* animals or N2 animals to examine the expression pattern. Both transgenic strains show identical expression.

RESULTS

ipp-5 encodes a type I 5-phosphatase homolog

To better understand regulation of IP_3 signaling, we sought to identify additional downstream genes involved in the LET-23 RTK mediated inositol 3,4,5-triphosphate (IP_3) signaling pathway for ovulation in *C. elegans* (Clandinin et al., 1998). Clandinin et al. (1998) identified *lfe-1*, an IP_3 receptor (IP_3R) homolog, and *lfe-2*, an IP_3 kinase (IP_3K) homolog, as suppressors of *lin-3(rf)* sterile ovulation defective mutants, indicating that ovulation is dependent on an evolutionary conserved IP_3 signaling pathway (Figure 1). Video analysis of *lfe-2* mutants shows no obvious ovulation defect (see Video 1), suggesting the inositol polyphosphate 5-phosphatase which also metabolizes IP_3 in other systems, may play a critical role inhibiting signaling in *C. elegans* ovulation. The *C. elegans* genome sequence predicts a single ortholog of the human type I **i**nositol **p**olyphosphate 5-**p**hosphatase (CO9B8.1), which we designate *ipp-5* (The *C. elegans* Sequencing Consortium, 1998). We sequenced a full-length *ipp-5* cDNA (kindly provided by Yuji Kohara) corresponding to this region, and found 11 nucleotides of an SL1 trans-spliced leader and a single ORF, comprising 7 exons which encode a 400 amino acid protein 42% identical to its human counterpart (Figure 2). The *C. elegans* IPP-5 lacks the well conserved motif (GDLNYRL) present in all members of the type II 5-phosphatases, as seen in the *C. elegans* homolog, C16C2.3 (Figure 2B). However, IPP-5 contains the conserved active site motif (PAWC/TDRV/ILM) essential for enzymatic activity of all type I and type II 5-phosphatases (Communi, 1996; Jefferson, and Majerus, 1996; Majerus, 1996; Erneux, 1998). On this basis, we classify IPP-5 as a type I phosphatase. IPP-5 lacks the C-terminal isoprenlylation site CCVVQ present in members of the 5-phosphatase type I family, suggesting that it relies on another mechanism for targeting to its correct intracellular location.

ipp-5 affects ovulation and fertility

To study *ipp-5* function, we isolated a deletion mutant, *ipp-5(sy605),* in which 240 bp upstream of the start codon is deleted through 28 bp of exon 3. We examined *ipp-5(sy605)* mutant animals for defective ovulation. There are no other obvious visible defects.

In a wild-type hermaphrodite, oocytes align on the proximal–distal axis of the gonadal sheath and mature in an assembly-line fashion as they proceed proximally towards the spermatheca. Typically, during ovulation, the sheath contracts and pulls the dilated spermatheca over the most proximal mature oocyte in the proximal gonad to release it from the oviduct into the spermatheca (McCarter et al., 1999). Animals with defects in ovulation have a reduced brood size. For example, analysis of Nomarski ovulation videos indicate *let-23(sa62)* RTK gain-of-function (gf) and *dec-4/itr-1* IP_3R reduction-of-function (rf) mutants show mechanical defects in ovulation (*dec-4(sa73),* n=20/20 defective ovulations; *let-23(sa62),* n=12/12 defective ovulations; see Videos 3 and 4) and have lower broods than wild type (mean brood 121 ± 9, see Figure 4B (Dal Santo et al., 1999); *let-23(sa62)* mean brood 173, range 45-276, n=24; Katz et al., 1996 In *sa62* mutants, the spermatheca constricts abnormally and tears the ovulated ooctye, leaving the nucleus behind in the gonad. The defect in *sa73* mutants is more pronounced; the basal sheath contraction rate in *sa73* mutants appears reduced relative to wild type, and the spermatheca dilates and constricts continually during ovulation before it finally pinches shut tearing the oocyte, leaving the nucleus behind. Furthermore, *lin-3(rf)* or *let-23(rf)* mutants are sterile (Aroian et al., 1991) because they fail to ovulate (Clandinin et al., 1998; McCarter et al., 1999).

Figure 3 shows a sequential image series of a wild type and a *sy605* hermaphrodite during ovulation (see Videos 2 and 5). The deletion mutant shows a novel ovulation phenotype whereby more than one oocyte is ovulated per cycle. In these double ovulations, the spermatheca dilates and extends beyond the proximal oocyte to precociously envelop the second and in some cases the third oocyte. In *sy605*, the spermatheca extends on average 49.1 ± 11.9 μm (n=18) compared to 33.9 ± 4.7 μm in the wild type (n=30; $p<0.0001$, Fisher's Exact Test). This observation indicates that IPP-5 is required to prevent excessive spermathecal dilation and extension during ovulation.

Prior work by McCarter et al. (1999) suggests ovulation is coupled to oocyte meiotic maturation. In *sy605* mutant animals, along with the proximal oocyte, the secondary oocyte is ovulated precociously, before the hallmarks of maturation are observed (McCarter et al, 1999). Presence of the nucleolus and nuclear envelope in these precocious oocytes indicate they have not undergone maturation (Figure 4). This mutant phenotype raises the possibility that there is no absolute requirement for an oocyte to have undergone maturation to be ovulated. In *ceh-18* mutants; immature oocytes are ovulated but do not appear to form zygotes (Rose et al., 1997). In *sy605*, the distal oocytes ovulated prior to maturation are apparently not fertilized, because we have seen oocytes interdigitating with fertilized multicellular eggs in the uterus (n=9). Video analysis of the fate of the secondary oocyte (ovulated precociously) indicate fertilization and embryogenesis does not ensue, as observed in the accompanied fertilized primary oocyte (n=11/11). Taken together, these results suggest that while meiotic maturation is not required for ovulation, it may be required for fertilization.

sy605 homozygotes have a reduced brood of 144 ± 20 (n=25) relative to the wild-type brood of 337 ± 33 (n=20, $p<0.001$; Table 1). Animals heterozygous for the deletion have a slightly reduced brood size (314 ± 36; n=20) relative to wild type ($p=0.0437$;

Table 1). Heterozygotes ovulate one oocyte/cycle (n=54) as do wild type, indicating the double ovulation phenotype is recessive.

To confirm that the deletion in the *ipp-5* locus causes the observed ovulation defect, we tested whether a transgene containing the full-length wild-type genomic *ipp-5* locus, including 2 kb sequence upstream of the start ATG codon, could complement the defect in *sy605* transgenic animals. In *sy605* animals, the ovulation defect is fully penetrant on a per animal basis (n=15/15 animals double ovulate); however, looking at successive ovulations in animals, we observe that every ovulation event is not mutant (49% of gonad arms ovulate one oocyte/cylce, n=70; Table 2B). Transgenic *sy605* animals bearing the *ipp-5* genomic locus as an extrachromosomal array showed rescue in all three lines examined (Table 2A). Thus, the ovulation defect is likely the result of the deletion, which removes *ipp-5* function, because the phenotype can be rescued by adding back wild-type copies of the *ipp-5* gene. It is conceivable that the next in-frame methionine downstream of the deletion, but upstream of the catalytic domain, initiates protein synthesis producing a protein. This protein which lacks the N terminal region, might result in altered protein activity, and thus the deletion might result in a gain-of-function phenotype. However, we think this possibility is inconsistent with our rescue data, and our genetic epistasis and interaction data in which *ipp-5(sy605)* behaves as a stronger version of *lfe-2*, which is a loss-of-function (see below). Thus, the simplest interpretation of the data is that *ipp-5(sy605)* is a loss-of-function mutation. Based on our mutant phenotype, we infer that IPP-5 likely regulates IP_3 signaling, which modulates spermathecal dilation/contraction.

IPP-5 acts in the adult spermatheca

To investigate where *ipp-5* might function, we examined the expression of a *ipp-5*::GFP transcriptional reporter. A 2 kb fusion of 5' sequence directed expression in the adult distal spermatheca and weakly in the proximal sheath in transgenic animals (Figure 5). This same promoter sequence driving the genomic *ipp-5* locus is sufficient to rescue the defect in *sy605* transgenic animals (Table 2A). To test whether expression in the spermatheca is sufficient for rescuing the ovulation defect, we used a heterologous spermathecal promoter (kindly provided by Alex Parker) to drive expression of the *ipp-5* cDNA. We observed rescue of the ovulation defect in two transgenic *sy605* lines observed. In *sy605* animals, 51% of the gonad arms examined were mutant where more than one oocyte was ovulated per cycle while 33% mutant gonad arms were observed in *sy605* animals bearing the transgene as an extrachromosomal array ($p<0.0246$). In a second line, 20% of the gonad arms were mutant ($p=0.0002$; Table 2B). Thus, expression of the transgene led to significantly more animals with normal ovulation, indicating expression of *ipp-5* in the spermatheca is sufficient to rescue the ovulation defect. While *ipp-5*::GFP expression is also detected in the vulva and isthmus of the pharynx throughout larval development and adulthood, we think it unlikely that expression in these tissues affects the spermathecal contraction behavior. Transgenic *sy605* worms injected with a transgene containing a sheath promoter (kindly provided by Anne Hart) driving the *ipp-5* cDNA did not show rescue of the ovulation defect in four lines observed (Table 2B). Together with the expression data, we infer *ipp-5* likely functions within the adult spermatheca to regulate ovulation.

We do not observe expression of the *ipp-5::GFP* reporter transgene before adulthood in the spermatheca, suggesting the function of *ipp-5* is needed in the adult spermatheca for ovulation rather than for the development or specification of the sheath

and spermatheca lineages, which occurs in the L4 larval stage (Kimble and Hirsh, 1979). We observed L4 stage *sy605* hermaphrodites under Nomarski optics and found that they had normal spermathecae and proximal sheath: the numbers of spermathecal cells were normal, and there was no obvious abnormality in spermathecal morphogenesis nor in the proximal ovarian sheath (n=13). To determine if expression of *ipp-5* in adult stage is sufficient for its function in ovulation, we examined whether using a heat shock promoter driving the *ipp-5* cDNA to induce expression in *sy605* adults is sufficient to rescue the ovulation defect. In two lines observed, induced expression of *ipp-5* function in adults was sufficient to rescue the double ovulation phenotype in transgenic *sy605* worms: (line-1) 22% mutant gonad arms after HS vs. 53% mutant gonad arms in control transgenic animals no HS, p= 0.0005; (line 2) 26% mutant gonad arms after HS vs. 49% mutant gonad arms in control transgenic animals no HS, p=0.0123 (Table 2C). We conclude that IPP-5 activity is not required before the L4 larval stage for its function in ovulation. The temporal and spatial regulation of *ipp-5* is consistent with its regulatory function during adult ovulation rather than in developmental processes that secondarily affect dilation.

ipp-5* suppresses the sterility of *lin-3* and *let-23

LIN-3 has been proposed to activate LET-23 and an IP_3 signaling pathway (Clandinin et al., 1998) that regulates ovulation. This pathway comprises *lin-3, let-23, lfe-1,* and *lfe-2* encoding an EGF-like growth factor, EGFR, IP_3R and IP_3K, respectively (Figure 1). *lin-3(rf)* and *let-23*(*rf)* mutants are sterile producing no progeny because they fail to ovulate. These mutants have an Emo phenotype in which the oocytes become trapped in the gonad arm and undergo multiple rounds of DNA synthesis (Clandinin et al., 1998; McCarter et al., 1999). A gain-of-function mutation in *lfe-1* IP_3R, or a loss-of-function mutation in *lfe-2* IP_3K, can bypass the requirement for wild-type levels of LET-23 activity: *lin-3(rf); lfe* or *let-23(rf); lfe* double mutants are fertile (Clandinin et al., 1998). We tested whether the *C. elegans* IPP-5 functions downstream of LET-23 RTK and can suppress the sterility of either *lin-3(rf)* or *let-23(rf). lin-3(n1058),* which affects vulva induction and fertility, has an average brood size of 0.2 ± 1.8 (n=76). In contrast, *lin-3(n1058); ipp-5(sy605)* double mutants are 98.7% fertile (n=319) having an average brood size of 28 ± 9, n=47 (Table 1); an allele of *lin-3, n378,* that affects only vulva induction (causing a vulvaless phenotype where the animals are unable to lay eggs), has an average brood size of 72 ± 11, n=17 (Clandinin et al., 1998). Similarly, *ipp-5* suppresses *let-23(rf),* as 100% of *let-23(sy10); ipp-5(sy605)* double mutants are fertile (n=21; Table 1). Because *sy605* can suppress the sterile defect of *lin-3* as well as *let-23,* we conclude that *ipp-5* functions downstream of *lin-3* and *let-23* to mediate ovulation.

***ipp-5* synergizes with other genes in the *let-23* mediated fertility pathway**

We next examined genetic interactions of *ipp-5* with known components of the fertility pathway. *lfe-1/itr-1(gf)* or *lfe-2(lf)* single mutants have a slightly reduced brood size and ovulate normally (Clandinin et al., 1998). *ipp-5* synergizes with either *lfe-1(gf)* or *lfe-2(lf)* to produce a synthetic sterile Emo phenotype (Figure 3) similar to that observed in *lfe-1(gf); lfe-2(lf)* double mutants (Clandinin et al., 1998) where the spermatheca fails to dilate sufficiently. *lfe-1(sy290); ipp-5* double mutants have an average brood of 6 ± 12 (n=55) compared to *lfe-1(sy290)* which has an average of 207 ± 35(n=26). *lfe-2(sy326)* has a brood of 213 ± 34 (n=23), whereas *lfe-2(sy326); ipp-5* double mutants are sterile

producing no progeny (n=86; Table 1). The data indicate that *ipp-5* interacts with both *lfe-1/itr-1* and *lfe-2* and that it likely functions in the adult spermatheca to regulate the fertility pathway during ovulation. Consistent with this hypothesis, all three proteins are expressed in the adult spermatheca (Clandinin et al., 1998; Dal Santo et al., 1999; Gower et al., 2001).

ipp-5(sy605) exhibits a semi-dominant synergistic effect in a sensitized background. Analysis of ovulation videos show that while *sy605/+* heterozygotes and *lfe-1* or *lfe-2* single mutants do not double ovulate, *sy605* heterozygotes that are also homozygous for *lfe-2* double ovulate and are fertile (n=17). Similarly, *sy605* heterozygotes that are also homozygous for *lfe-1* are fertile and double ovulate (n=10). *sy605* synergizes with *lfe-1* and *lfe-2* mutations in a dose sensitive manner, because removing two copies of *ipp-5* has more severe affects than removing a single copy. The Emo phenotype observed in the *lin-3(rf)* or *let-23 (rf)* single mutant and double mutant *ipp-5*; *lfe-1* or *ipp-5; lfe-2,* suggests IP_3 signaling levels are critical for normal hermaphrodite ovulation and fertility. From our study on *ipp-5* mutant phentotypes, we infer that IPP-5 inhibits IP_3 signaling after activation to ensure ovulation occurs properly.

To further examine the affects of varying IP_3 signaling on ovulation, we examined double mutants of *ipp-5* with a gain-of-function allele of *let-23(sa62*) RTK (Katz et al., 1996). *sa62* animals have a reduced brood which may in part be attributed to the sickness of the homozygotes (average brood 173, range 24-276 progeny, n=24; Katz et al., 1996), and an ovulation defect where the spermathecal valve contracts prematurely, closing and tearing the oocyte as it enters (n=12; see Video 4). *ipp-5* also synergizes with *sa6*2, causing a further reduction in brood size (average brood 7; range 0-27 progeny; n=31). In these double mutants, the spermatheca extends beyond the proximal oocyte to the second oocyte; but it then retracts, and has problems ovulating the proximal oocyte and eventually causes an Emo phenotype (n=8). Precise control of IP_3 levels appears to be crucial *in vivo* for proper spermathecal dilation. Thus, both insufficient and excessive IP_3 signaling cause defective ovulation.

IPP-5 and LFE-2 have different roles in regulating IP3 signaling

Both the 5-phosphatase and 3-kinase metabolize IP_3; however, their respective contributions in negatively regulating IP_3 signaling are unclear. Clandinin et al. showed that *lfe-2(sy326)* mutation disrupts kinase activity since it failed to phosphorylate IP_3 in an in vitro kinase assay (Clandinin et al, 1998). The point mutation in *lfe-2* and the deletion in *ipp-5* are probably loss-of-function mutations. We examined the ovulation phenotype of both these alleles by Nomarski video analysis (see Videos 1 and 5). Although *lfe-2(lf)* mutants display a reduced brood size, video analysis shows no obvious defects in ovulation (n=22), unlike *ipp-5(sy605).* Strikingly, these genes, both of which likely regulate IP_3 levels, have qualitatively different loss of function phenotypes. We infer that IPP-5 and LFE-2 are both critical for ovulation but act differently to regulate it. We observe no effect with misexpression of IPP-5 in wild-type worms (unpublished observations); however, misexpression of LFE-2 using a heat shock promoter causes the spermatheca to relax inappropriately (Clandinin et al, 1998). The existence of multiple proteins that differentially inhibit IP_3 signaling highlight the importance of maintaining fine control of IP_3 signaling in ovulation.

DISCUSSION

In an attempt to better understand how IP_3 signaling downstream of the LET-23 RTK pathway affects ovulation and fertility, we have generated and characterized a deletion mutant of the *C. elegans* type I inositol polyphosphate 5-phosphatase. *ipp-5(sy605)* homozygous mutants have reduced fertility and a novel ovulation phenotype whereby the spermatheca dilates and extends abnormally. Epistasis analyses place *ipp-5* downstream of *let-23*. Two mutant loci have previously been identified which can bypass LET-23 RTK function, ***l***et-23 ***f***ertility ***e****ffectors, lfe-1(gf)/itr-1,* an IP_3 Receptor homolog, a positive effector, and *lfe-2(lf),* an IP_3 Kinase, a negative effector (Clandinin et al, 1998). *ipp-5(sy605)* enhances *lfe-1(gf)* and *lfe-2(lf)* mutants, causing sterility. Our transgenic rescue data (Table 2) and reporter GFP expression data (Figure 5) are consistent with IPP-5 directly controlling contraction and dilation behavior in the adult spermatheca (Figure 1).

Contributions of the 5-phosphatase and IP_3 kinase and negative regulation of IP_3 signaling

We observed that the *C. elegans* 5-phosphatase deletion mutant, *ipp-5(sy605),* and the IP_3 kinase mutant, *lfe-2(lf),* have qualitatively different ovulation phenotypes. The double ovulation phenotype of *ipp-5* probably results from increased IP_3 signaling upon removing IPP-5 function. Consistent with this, cell lines that stably underexpress a type I 5-phosphatase have a sustained 2.6 fold elevation in IP_3 leading to enhanced intracellular calcium oscillations and cellular transformation (Speed et al., 1996; 1999; 2000). By contrast, *lfe-2(lf)* shows no noticeable ovulation defect in *C. elegans*. We infer that eliminating activity of either gene allows IP_3 to accumulate to different levels resulting in the two distinct phenotypes, suggesting they have distinct negative regulatory roles within the context of ovulation. Studies of IP_3 metabolism in *Xenopus* oocytes indicate that at low [IP_3] and high [Ca^{2+}], IP_3 is metabolized predominantly by IP_3K, while as [IP_3] increases, the 5-phosphatase degrades progressively more IP_3 irrespective of the [Ca^{2+}] (Sims et al., 1996). Multiple enzymes that metabolize IP_3 imply tight regulation of IP_3 is essential for ensuring proper spermathecal dilation/relaxation during ovulation. In *C. elegans*, elevated IP_3 signaling affects spermathecal dilation, and IPP-5 is critical for inhibiting signaling for contraction.

Ovulation is regulated by IP_3 signaling levels

Cell culture studies have shown the mammalian 5-phosphatase and IP_3 kinase metabolize IP_3 into either IP_2 or IP_4, respectively (Irvine et al., 1986; Berridge, 1989). Simultaneously removing *ipp-5* activity and *lfe-2* activity should create a situation where IP_3 accumulates and exerts negative feedback inhibition which blocks further ovulation.

We interpret the effects on spermathecal dilation in the *lfe-2; ipp-5* mutant as being mediated through either too low or excessively high levels of IP_3 signaling. Moreover, a double mutant with *ipp-5* and *sa62*, a gain-of-function allele of *let-23* RTK (Katz et al., 1996), which has hyperactive signaling, also shows the same ovulation defect, further demonstrating the inhibitory effects of excessive IP_3 signaling. Cell culture studies have shown that epidermal growth factor stimulates IP_3 production and a rise in intracellular calcium (Hepler et al., 1987). An activating mutation in LET-23 RTK likely results in higher levels of second messenger IP_3 production. We presume that the cooperative effect of removing IPP-5 in the gain-of-function LET-23 mutant dramatically increases IP_3 signaling, which prevents ovulation causing the Emo phenotype.

Examining the spermatheca in these mutants allows us to see a more direct physiological effect of perturbing IP_3 signaling *in vivo*. There appears to be a biphasic phenotypic effect on the extent of spermathecal dilation and extension with increasing levels of IP_3 signaling in *C. elegans*. In *lin-3(rf)* and *let-23(rf)* mutants with reduced EGF signaling, IP_3 signaling is not sufficient for the spermatheca to dilate. In *ipp-5* mutants where IP_3 signaling is higher, the spermatheca dilates and extends farther than in the wild type to ovulate the proximal mature oocyte along with the secondary distal oocyte, which has not undergone meiotic maturation. One explanation for this observation is that in *sy605*, the proximal oocyte, which has undergone meiotic maturation, triggers the spermatheca to dilate. The secondary distal oocyte is passively ovulated precociously, as a consequence of the spermatheca extension beyond the proximal oocyte due to increased IP_3 signaling.

Further elevations in IP_3 signaling in various double mutants prevent spermatheca dilation. IP_3 positively effects gating of IP_3R, but has also been shown along with calcium to exert negative feedback, which may explain this phenotype (Berridge, 1993; Ehrlich and Watras, 1988; Besprozvanny, 1991). Multiple layers of regulating intracellular calcium release allows fine control of many cellular processes.

LET-23 RTK induced activation of IP_3 signaling which promotes spermatheca dilation, likely through its effect on calcium release, is reminiscent of arterial smooth muscle relaxation and arterial dilation by calcium sparks (Nelson et al., 1995). The structural architecture of the myoepithelial sheath and spermatheca resemble smooth muscle. Longitudinal interdigitated thick and thin filaments make up the sheath. Actin stains the spermatheca, revealing circumferentially arranged fibers (Strome, 1986) that may undergo peristaltic vasoconstrictive and dilatory behavior like that of epithelial smooth muscle. The tension from the contracting sheath pulls the dilated spermatheca over the proximal oocyte during ovulation (McCarter, 1999). Decreases in IP_3 signaling may trigger contraction and closure of the distal spermatheca valve so that only one oocyte is enveloped. A peristaltic wave of contraction may carry the oocyte from the distal spermatheca valve through the proximal spermathecal valve into the uterus.

Ovulation is a regulated behavior requiring coordination of the epithelial smooth muscle-like spermatheca and sheath. Animals with defective ovulation have reduced fertility, thus proper regulation of ovulation is important for normal fertility. During ovulation, we propose IPP-5 is necessary to prevent spermathecal hyperextension by negatively regulating IP_3 signaling downstream of RTK, thereby ensuring proper spermathecal dilation and contraction behavior.

Acknowledgments

We thank Y.Hadju-Cronin, J.Copeland, and B.Bingol for help isolating *sy605;* Y. Kohara for cDNA; J.Thomas for *sa62* and *sa73;* A. Fire for GFP and HS vectors; A. Parker for the *pCeh* promoter and strain KR3738; A. Hart for the *nlp-8* promoter and strain PT4; L.R. Garcia, E. Schwarz, other members of our lab, and an anonymous reviewer for valuable discussion and comments on the manuscript; and L. Maxfield (Caltech Digital Media Center) for help making web movies. The *Caenorhabditis* Genetics Center provided some strains. This project was supported by the HHMI, with which P.W.S is an investigator. Y.K.B. is a NIH trainee supported by NIH 5T32GM07737.

GenBank Accession Number

The GenBank accession number for the full-length *ipp-5* cDNA nucleotide sequence is AF411588.

REFERENCES

Aroian, R., and Sternberg, P. (1991). Multiple functions of *let-23*, a *Caenorhabditis elegans* receptor tyrosine kinase gene product required for vulva induction. Genetics *128*, 251-267.

Berridge, M.J. and Irvine, R.E. (1984). Inostiol triphosphate, a novel second messenger in cellular signal transduction. Nature *31*, 315-321.

Berridge, M.J. and Irvine, R.E. (1989). Inositol phosphates and cell signaling. Nature *341*, 197-205.

Berridge, M.J. (1993). Inositol triphosphate and calcium signaling. Nature *361*, 315-325.

Berridge, M.J. (1995). Calcium signaling and cell proliferation. Bioessays *17*, 491-500.

Besprozvanny, I., Waras, J., and Ehrlich, B.E. (1991). Bell-shaped calcium response curves on Ins(1,4,5)P_3 and calcium-gated channels from endoplasmic reticulum of cerebellum. Nature *351*, 751-754.

Bootman, M.D. and Berridge J.M. (1995). The elemental principles of calcium signaling. Cell *83*, 675-678.

Brenner, S. (1974). The genetics of *Caenorhabditis elegans*. Genetics *77*, 71-94.

The *C. elegans* Sequencing Consortium. (1998). Genome sequence of the nematode *C. elegans:* A platform for investigating biology. Science *282*, 2012-2018

Clandinin, T.R., DeModena, J.A., and Sternberg, P.W. (1998). Inositol triphosphate mediates a ras- independent response to LET-23 receptor tyrosine kinase activation in *C. elegans*. Cell *92*, 523-533.

Clapham. D.E. (1995). Calcium signaling. Cell *80*, 259-268.

Communi D., Lecocq R., Erneux C. (1996). Arginine 343 and 350 are two active residues involved in substrate binding by human type I D-myo-inositol 1,4,5,-trisphosphate 5-phosphatase. J Biol. Chem *271*, 11676-83.

Cremona O, Di Paolo G, Wenk MR, Luthi A, Kim W.T, Takei K, Daniell L, Nemoto Y, Shears SB, Flavell RA, McCormick DA, De Camilli P. (1999). Essential role of phosphoinositide metabolism in synaptic vesicle recycling. Cell *99*, 179-88.

Dal Santo, P., Logan, M.A., Chisholm, A.D., Jorgensen, E.M. (1999). The inositol triphosphate receptor regulates a 50-second behavioral rhythm in *C. elegans*. Cell *98*, 757-767.

Drayer AL, Pesesse X, De Smedt F, Communi D, Moreau C, Erneux C. (1996). The Family of inositol and phosphatidyl polyphosphate 5-phosphatasaes. Biochem Soc. Trans *24*, 1001-5.

Ehrlich B.E., Watras J. (1988). Inositol 1,4,5-trisphosphate activates a channel from smooth muscle sarcoplasmic reticulum. Nature *336*, 583-6.

Erneux C., Govaerts C., Communi D., Pesesse X. (1998). The diversity and possible functions of the inositol polyphosphate 5-phosphatases. Biochim Biophys Acta. *1436*, 185-99.

Ferguson E.L, Horvitz H.R. (1985). Identification and characterization of 22 genes that affect the vulval cell lineages of the nematode *C. elegans.* Genetics *110*, 17-72.

Fodor, A., and Deak, P. (1985). The isolation and genetic analysis of a C. elegans translocation (szT1) strain bearing an X-chromosome balancer. Journal of Genetics *64*, 143-157.

Gower, N.J.D., Temple, G.R., Schein, J.E., Marra, M.A., Walker, D.S. Baylis, H.A. (2001). Dissection of the promoter region of the inositol 1,4,5-triphosphate receptor gene, itr-1, in *C. elegans*: A molecular basis for cell-specific expression of IP3R isoforms. JMB *306*, 145-157.

Helgason C.D., Damen J.E., Rosten P., Grewal R., Sorensen P., Chappel S.M., Borowski A., Jirik F., Krystal G., Humphries R.K. (1998). Targeted disruption of SHIP leads to hemopoietic perturbations, lung pathology, and a shortened life span. Genes Dev. *12*, 1610-20.

Hepler JR, Nakahata N, Lovenberg TW, DiGuiseppi J, Herman B, Earp HS, Harden TK. (1987). Epidermal growth factor stimulates the rapid accumulation of inositol (1,4,5) triphosphate and a rise in cytosolic calcium mobilized from intracellular stores in A431 cells. J. Biol. Chem. *262*, 2951-2956.

Irvine, R.F., Letcher, A.J., Heslop, J.P., Berridge, M.J. (1986). The inositol tris/tetrakisphosphate pathway- demonstration of Ins (1,4,5) P_3 3-kinase activity in animal tissues. Nature *320*, 631-4.

Iwasaki K, Liu D.W.C, Thomas J.H. (1995). Genes that control a temperature-compensated ultradian clock in *Caenorhabditis elegans*. PNAS *92*, 10317-10321.

Janne P.A., Suchy S.F., Bernard D., MacDonald M., Crawley J., Grinberg A., Wynshaw-Boris A., Westphal H., Nussbaum R. L. (1998). Functional overlap between murine Inpp5b and Ocrl1 may explain why deficiency of the murine ortholog for OCRL1 does not cause Lowe syndrome in mice. J Clin Invest. *101*, 2042-53.

Jefferson, A.B., and Majerus, P.W. Mutation of the conserved domains of two inositol polyphosphate 5-phosphatases. Biochemistry J. *35*, 7890-7894.

Katz WS, Lesa GM, Yannoukakos D, Clandinin TR, Schlessinger J, Sternberg PW. (1996). A point mutation in the extracellular domain activates LET-23, the *Caenorhabditis elegans* epidermal growth factor receptor homolog. Mol. Cell Biol. *16*, 529-537.

Kimble, J., and Hirsh, D. (1979). Postembryonic cell lineages of the hermaphrodite and male gonads in *Caenorhabditis elegans.* Dev. Bio. *70*, 396-417.

Laxminaryayan, K.M., Matzaris, M., Speed, C.J., Mitchell, C.A. (1993). Purification and characterization of a 43-kDa membrane-associated inositol polyphosphate 5-phosphatase from human placenta. J. Biol. Chem. *268*, 4968-4974.

Majerus, P.W. (1992). Inositol phosphate biochemistry. Annu. Rev. Biochem. *61*, 225-250.

Majerus, P.W. (1996). Inositols do it all. Genes Dev *10*, 1051-1053.

McCarter J., Bartlett B., Dang T., Schedl T. (1999). On the control of oocyte meiotic maturation and ovulation in *Caenorhabditis elegans*. Dev. Bio. *205*, 111-128.

Mello, C.C., Kramer, J.M., Stinchocomb, F., and Ambros, V. (1991). Efficient gene transfer in *C. elegans* extrachormosomal maintenance and integration of transforming sequences. EMBO J. *10*, 3959-3970.

Mitchell, C.A., Brown, S., Campell, J.K., Munday, A.D., and Speed, C.J. (1996). Regulation of second messengers by the inositol polyphosphate 5- phosphatases. Biochem Soc. Trans. *24*, 994-1000.

Nathoo AN, Moeller RA, Westlund BA, Hart AC. (2001). Identification of neuropeptide-like protein gene families in Caenorhabditiselegans and other species. Proc Natl Acad Sci U S A. *98(24):*14000-5.

Nelson M.T., Cheng H., Rubart M., Santana L.F., Bonev A.D., Knot H.J., Lederer W. J. (1995). Relaxation of arterial smooth muscle by calcium sparks. Science *270*, 633-637.

Rose KL, Winfrey VP, Hoffman LH, Hall DH, Furuta T, Greenstein D. (1997). The POU gene ceh-18 promotes gonadal sheath cell differentiation and function required for meiotic maturation and ovulation in Caenorhabditis elegans. Dev Biol. *192* (1), 59-77.

Sambrook J., Fristch, E.F., and Maniatis, T. (1989). Molecular Cloning: A Laboratory Manual, Second Edition. Cold Spring Harbor, NY: Cold Spring Harbor Laboratory Press.

Sims C.E., and Allbritton, N.L. (1998). Metabolism of inositol 1,4,5-triphoshate and inositol 1,3,4,5-tetrakisphosphate by the oocytes of Xenopus laevis. J. Biol. Chem. *273*, 4052-4058.

Speed, C.J., Little, P.J., Hayman, J.A., and Mitchell, C.A. (1996). Underexpression of the 43 kDa inositol polyphosphate 5-phosphatase is associated with cellular transformation. EMBO J. *15*, 4852-4861.

Speed, C.J., Naylon, C.B., Little, P.J., and Mitchell, C.A. (1999). Underexpression of the 43 kDa inositol polyphosphate 5-phosphatase is associated with spontaneous calcium oscillations and enhanced responses following endothelin-1 stimulation. J. Cell. Science *112*, 669-679.

Speed, C.J., and Mitchell, C.A. (2000). Sustained elevation in inositol 1,4,5-triphosphate results in inhibition of phosphatidylinositol transfer protein activity and chronic depletion of the agonist sensitive phosphoinositide pool. J. Cell Science *113*, 2631-2636.

Stolz L.E., Huynh C.V., Thorner J., York J.D. (1998). Identification and characterization of an essential family of inositol polyphosphate 5-phosphatases (INP51, INP52 and INP53 gene products) in the yeast *Saccharomyces cerevisiae*. Genetics *148*, 1715-29.

Strome, S. (1986). Fluorescence visualization of the distribution of microfilaments in gonads and early embryos of the nematode *C. elegans.* J. Cell Biol. *103*, 2241-2252.

Verjans, B., Lecocq, R., Moreau, C., Erneux, C. (1992). Purification of bovine brain inositol-1,4,5-trisphosphate 5-phosphatase. Eur. J. Biochem *204*, 1083-1087.

Table 1. *ipp-5(sy605)* suppresses the sterility of *lin-3(rf)* and *let-23(rf)* and synergizes with other genes in the *let-23*-mediated fertility pathway. Fertile is defined as having greater than five offspring. Alleles used are *lin-3(n1058), let-23(sy10), lfe-1(sy290), lfe-2(sy326),* and *let-23(sa62). unc-4(e120)* was used as a marker and *mnC1[dpy-10(e128) unc-52(e444)]* as a balancer for *let-23* while *unc-24(e138)* was used as a marker and *DnT1[nT1[unc(n745dm)let]* as a balancer for *lin-3. lfe-1* was marked with *unc-24(e138)* and *lfe-2* marked with *unc-57(ad592). *sy10* animals display a partially penetrent larval lethal phenotype associated with *let-23(rf)* decreases in RAS signaling, thus broods were not determined.

Table 2. Transgenic assay for rescue of *ipp-5(sy605)* ovulation defect.
(A) During ovulation in wild-type animals the spermatheca envelops one oocyte. In *ipp-5(sy605)* animals, the spermatheca ovulates two and sometimes three oocytes at a time. A 2 kb sequence upstream of the ATG along with the entire genomic *ipp-5* locus rescues the phenotype when injected as a transgene in *sy605* animals (3/3 lines rescued).
(B) Site of action experiments. A heterologous spermatheca promoter, pCeh (provided by Alex Parker), fused to the *ipp-5* cDNA also rescues the defect in *sy605* transgenic animals (2/2 lines rescued) whereas the *nlp-8* sheath specific promoter (Anne Hart, personal comm.) does not (0/4 lines rescued). (C) A heat shock promoter driving expression of *ipp-5* cDNA in adults rescues the ovulation defect (2/2 lines rescued).

Figure 1. IP_3 mediated ovulation pathway.
Ovulation is dependent on an IP_3 mediated pathway that is activated by LIN-3 EGF and LET-23 EGFR, which likely stimulates hydrolysis of PIP_2 into IP_3. LFE-1 encodes an IP_3 Receptor homolog, which plays a known role in releasing intracellular calcium. LFE-2 encodes and IP_3 kinase that phosphorylates IP_3 into IP_4 (Clandinin et al., 1998). IPP-5 encodes a 5-phosphatase (5-Ptase), which likely dephosphorylates IP_3 into IP_2.

Figure 2. Molecular characterization of *ipp-5.*
(A) Genomic structure of *ipp-5.* CO9B8.1 corresponds to the predicted ORF, determined by the Genefinder Program, to encode a *C. elegans* homolog of the inositol

polyphosphate 5- phosphatase. Exons are shown as white boxes. The sequence is inferred from the cDNA (generously provided by Y. Kohara). The numbers above each intron indicate the base pair position relative to itself. The indicated region deleted in *sy605* spans 240 bp upstream of the start ATG codon through exon 3. (B**)** Protein sequence alignment of the *Drosophila,* dog, human and *C. elegans* homologs of the type I inositol 5-phosphatase and the *C. elegans* and human homologs of the type II 5-phosphatase. A *Drosophila* homolog has not been identified genetically, but Genie has predicted an ORF (GenBank accession AAF56383) in the sequenced genome. Identical residues are darkly shaded, while conserved substitutions are lightly shaded. The signature motif present in all 5-phosphatase family members is underlined in black. The motif well conserved among all type II phosphatases is double underlined. The residues deleted in *ipp-5* are indicated by a dashed underline.

Figure 3. *ipp-5(sy 605)* Effects on ovulation.
Still frame series of Nomarski photomicrographs of a hermaphrodite (A, B, C) wild type and (D, E, F) *ipp-5* gonad during ovulation. The wild-type images have been flipped horizontally so the orientation matches that of the *ipp-5* images. The uterus is towards the left and the proximal gonad is towards the right. The *ipp-5* phenotype shows two oocytes, indicated by white arrowheads, being ovulated in the spermatheca per cycle. See Supplementary Information Videos 2 and 5. Nomarski photomicrographs of (G) *lfe-1/itr-1; ipp-5* and (H) *lfe-2; ipp-5.* Double mutants between *ipp-5* and *lfe-X* cause the endomitotic oocyte nuclei (Emo) phenotype, indicated by black arrowheads. "Sp" denotes the position of the spermatheca while "Oo" denotes the oocyte. Animals were photographed using a 100X objective and DIC optics. Scale bar, 20 μm.

Figure 4. Fate of secondary oocyte in *ipp-5(sy605)* animals.
In *sy605* mutants, the second oocyte is ovulated along with the proximal oocyte and passed into the uterus. The secondary oocyte has not undergone maturation as the nucleolus (arrowhead) and the nuclear envelope (arrow) are still present. The proximal oocyte that was ovulated is at the one cell (1c) stage. A two-cell embryo is also shown (2c). Scale bar, 20 μm.

Figure 5. Expression of *ipp-5.*

Nomarski photomicrographs of a transgenic worm and their corresponding GFP fluorescence photomicrographs. The white arrowhead indicates position of the distal spermatheca while the white arrow indicates the sheath. Panels (A) and (B) show a worm before ovulation. Panels (C) and (D) show a transgenic *sy605* worm during ovulation. The arrowhead indicates the distal spermatheca enclosing two oocytes in a *sy605* transgenic animal. Strong expression is detected in the distal spermatheca while faint expression is detected in the sheath. Fertilized embryos are to the left while oocytes lining up in the proximal gonad are to the right. Scale bar, 20 μm.

Movies "Sp" denotes spermatheca, "Oo" denotes oocyte, "nu" denotes oocyte nucleus

Movie 1 *lfe-2* reduction-of-function mutant in IP_3 kinase recorded ovulation sequence. Ovulation proceeds essentially normally.

Movie 2 recorded sequence of wild type ovulation. During ovulation, the spermatheca dilates to envelop the proximal oocyte.

Movie 3 *dec-4(sa73)* reduction-of-function mutant in IP_3 Receptor recorded ovulation sequence. The spermatheca dilates and constricts continuously throughout ovulation, before finally tearing the proximal oocyte it passes into the spermatheca, leaving behind a portion with the nucleus in the gonad.

Movie 4 *let-23(sa62)* gain-of-function mutant in receptor tyrosine kinase recorded ovulation sequence. The spermatheca pinches early and tears the primary oocyte as it is being enveloped, leaving behind the nucleus in the gonad.

Movie 5 *ipp-5 (sy605)* loss-of-function mutant in 5-phosphatase recorded ovulation sequence. The spermatheca dilates and hyperextends to ovulate the proximal mature oocyte, and the secondary distal oocyte precociously along with it.

Table 1 *ipp-5(sy605)* suppresses the sterility of *lin-3(rf)* and let-23(rf) and synergizes with other genes in the *let-23*-mediated fertility pathway

Genotype Other	*ipp-5*	% fertile	n	brood
wild type	+/+	100%	20	337 ± 33
let-23(rf)	+/+	0%	40	0
lin-3(rf)	+/+	1.3%	76	0.2 ± 1.8
ipp-5/ipp-5	*sy605/sy605*	100%	25	144 ± 20
ipp-5/+	*sy605/+*	100%	20	314 ± 36
let-23(rf)	*sy605/sy605*	100%	21	n.d.*
lin-3(rf)	*sy605/sy605*	98.7%	319	28 ± 9 (n=47)
lfe-1(gf)	+/+	100%	26	207 ± 35
lfe-2(lf)	+/+	100%	23	213 ± 34
lfe-1(gf)	*sy605/sy605*	24%	55	6.0 ± 12
lfe-2(lf)	*sy605/sy605*	0%	86	0

Table 2 In vivo transgenic assay for rescue of *ipp-5(sy605)* ovulation defect

ipp-5 genotype	transgene	line #	conditions	% gonad arms 1 oocyte ovulated/cycle	% gonad arms 2 oocytes ovulated/cycle		n # gonad arms
A. Rescue by genomic *ipp-5* DNA							
+	-----			100 %	0 %		43
sy605	-----			0 %	100 %		15
sy605	*ipp-5*	1		74 %	26 %	p<0.0001	57
sy605	*ipp-5*	2		73 %	27 %	p<0.0001	51
sy605	*ipp-5*	3		66 %	34 %	p<0.0001	32
B. Site of Action. 1. pCEH spermtheca promoter driving *ipp-5* cDNA is sufficient for rescue							
sy605	-----			49 %	51 %		70
sy605	*pCEH::ipp-5*	23.1		67 %	33%	p=0.0246	93
sy605	*pCEH::ipp-5*	9.1		80 %	20 %	p=0.0002	65
2. *nlp-8* sheath promoter driving *ipp-5* cDNA is not sufficient for rescue							
sy605	-----			49 %	51 %		70
sy605	*nlp-8::ipp-5*	4.1		47 %	53 %	p=0.8685	77
sy605	*nlp-8::ipp-5*	10.1		40 %	60 %	p=0.3780	60
sy605	*nlp-8::ipp-5*	1.2		35 %	65 %	p=0.1930	51
sy605	*nlp-8::ipp-5*	1.1		47%	53 %	p=1.000	76
C. Heat shock induced expression of *ipp-5* cDNA in young adults is sufficient for rescue							
sy605	*hs::ipp-5*	18.2	no HS	47 %	53 %		51
sy605	*hs::ipp-5*	18.2	+ HS	78 %	22%	p=0.0005	78
sy605	*hs::ipp-5*	22.1	no HS	51 %	49 %		53
sy605	*hs::ipp-5*	22.1	+ HS	74 %	26 %	p=0.0123	66

Figure 1 IP_3 -mediated ovulation pathway

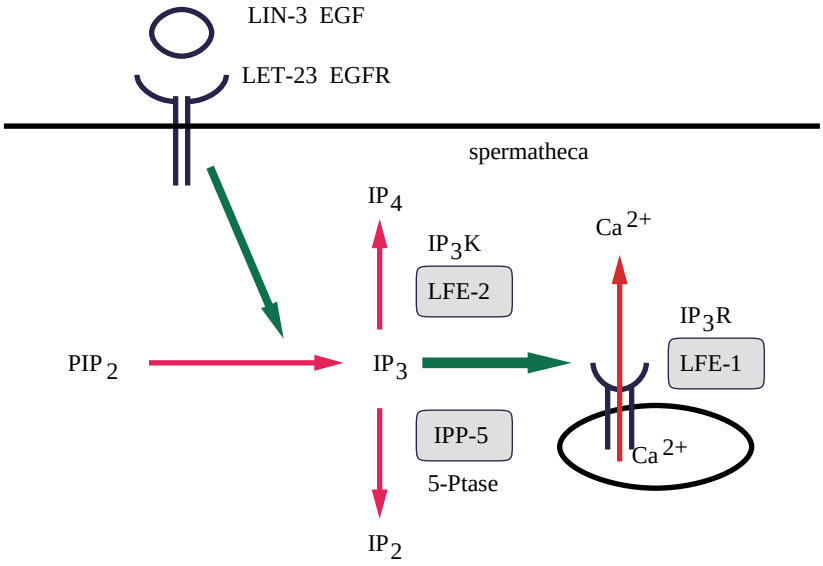

Figure 2A

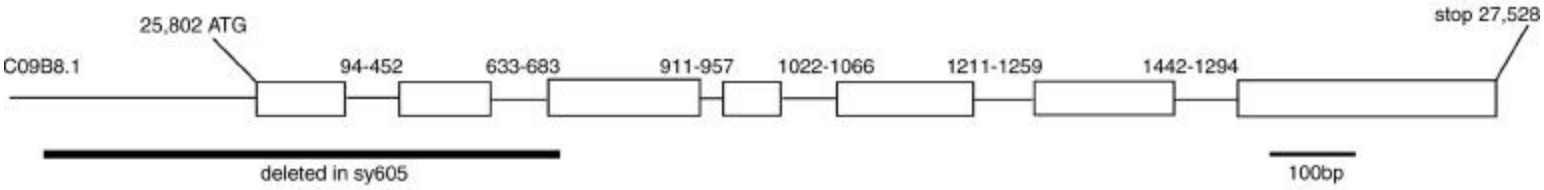
25,802 ATG
stop 27,528
C09B8.1
94-452
633-683
911-957
1022-1066
1211-1259
1442-1294
deleted in sy605
100bp

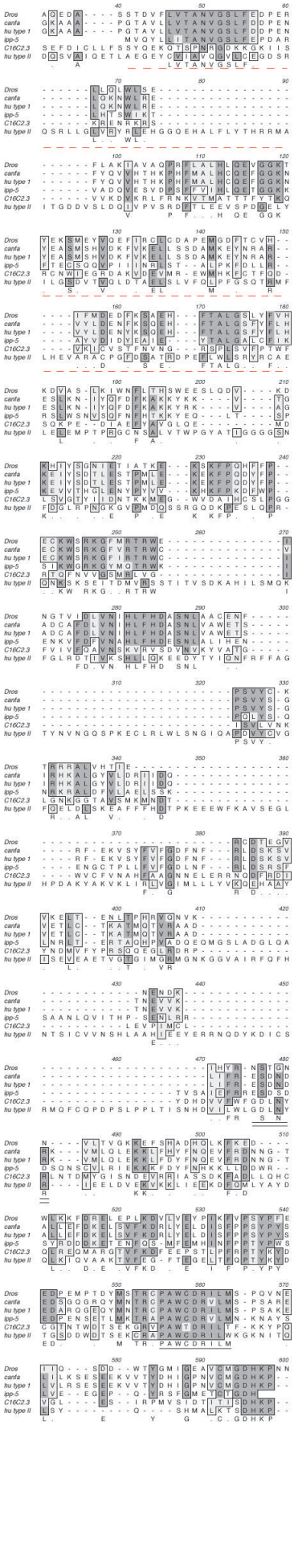
Dros
canfa
hu type I
ipp-5
C16C2.3
hu type II

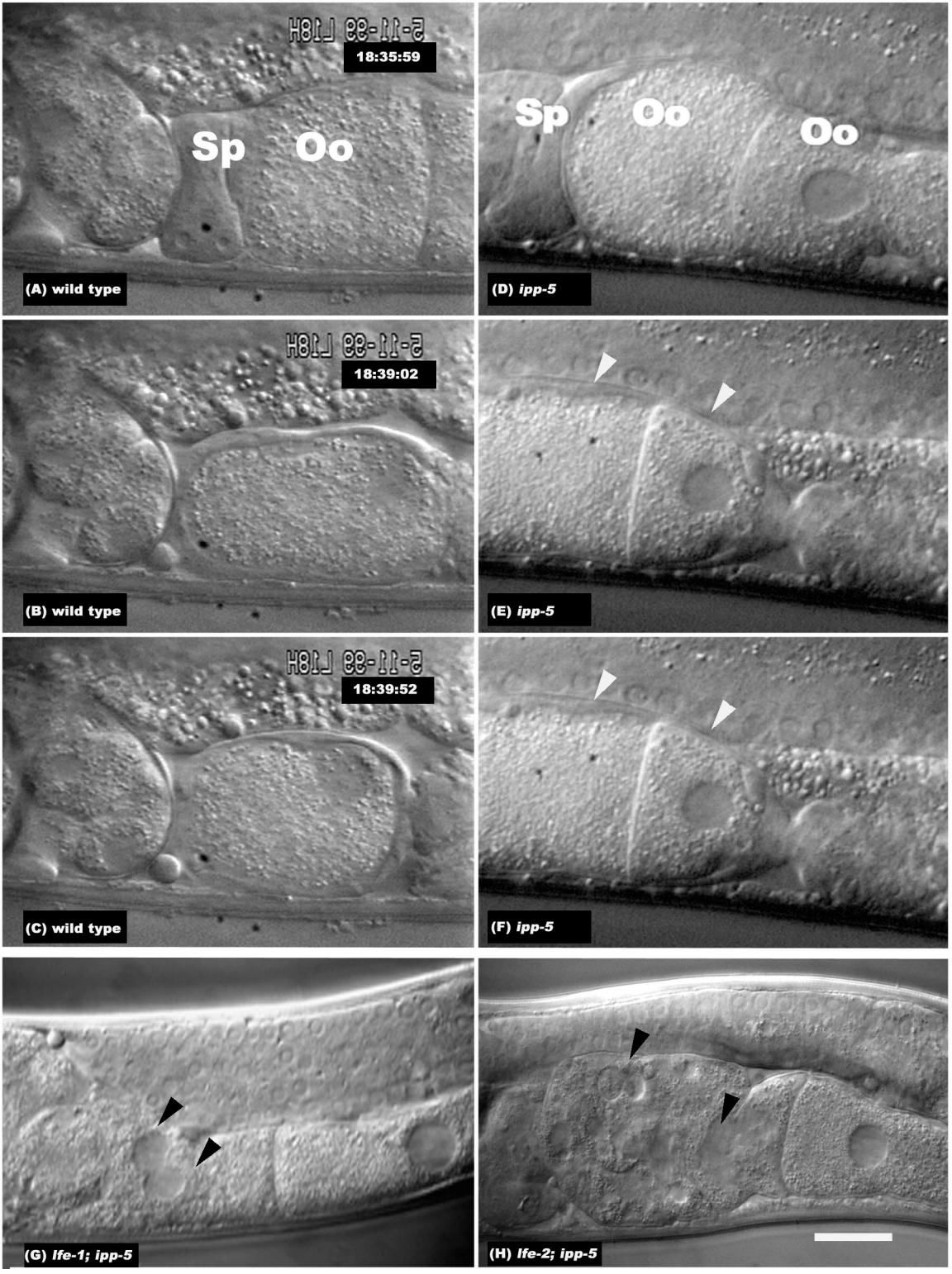
18:35:59
Sp
Oo
(A) wild type
Sp
Oo
Oo
(D) ipp-5
18:39:02
(B) wild type
(E) ipp-5
18:39:52
(C) wild type
(F) ipp-5
(G) lfe-1; ipp-5
(H) lfe-2; ipp-5

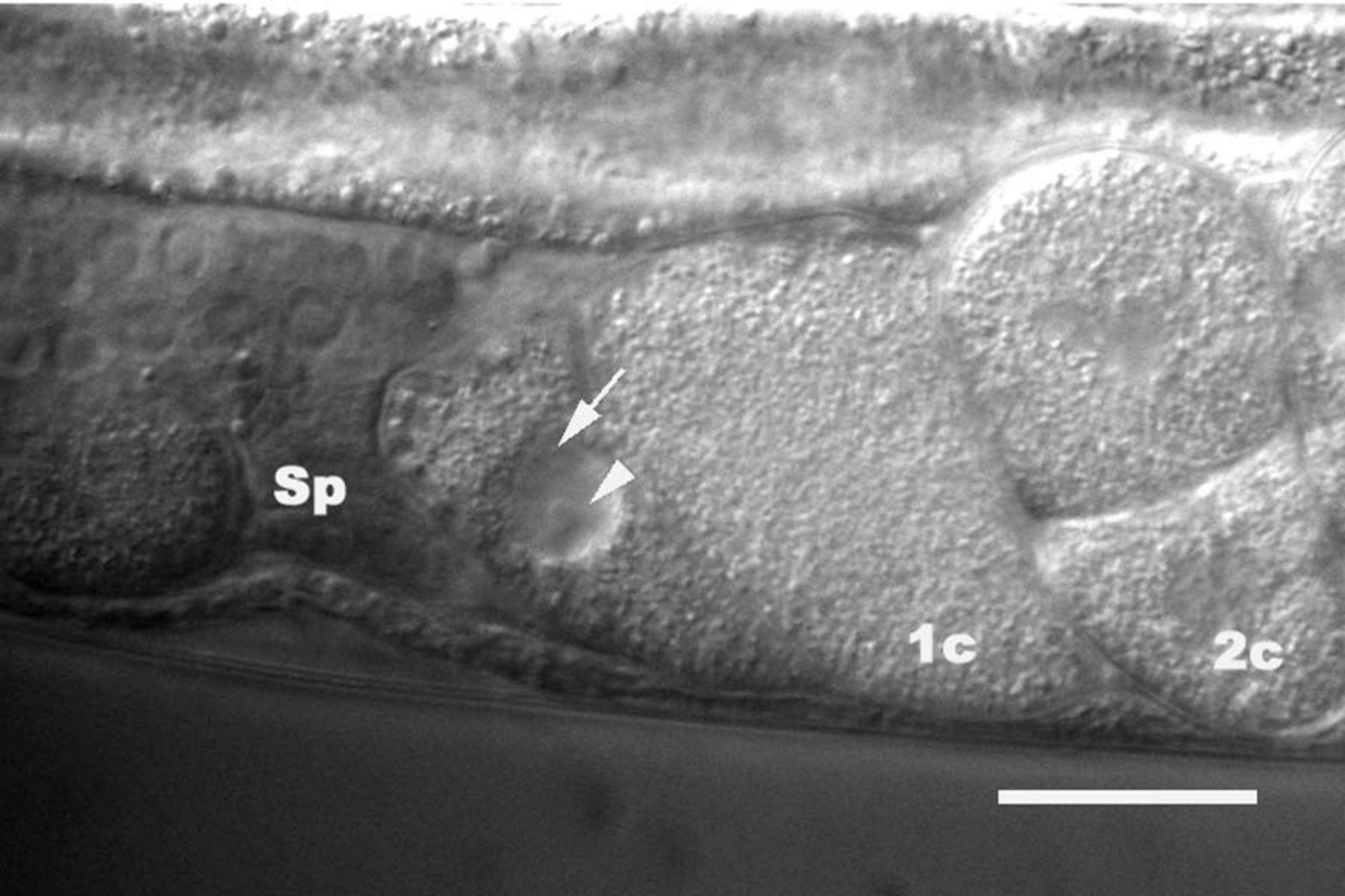
Sp
1c
2c

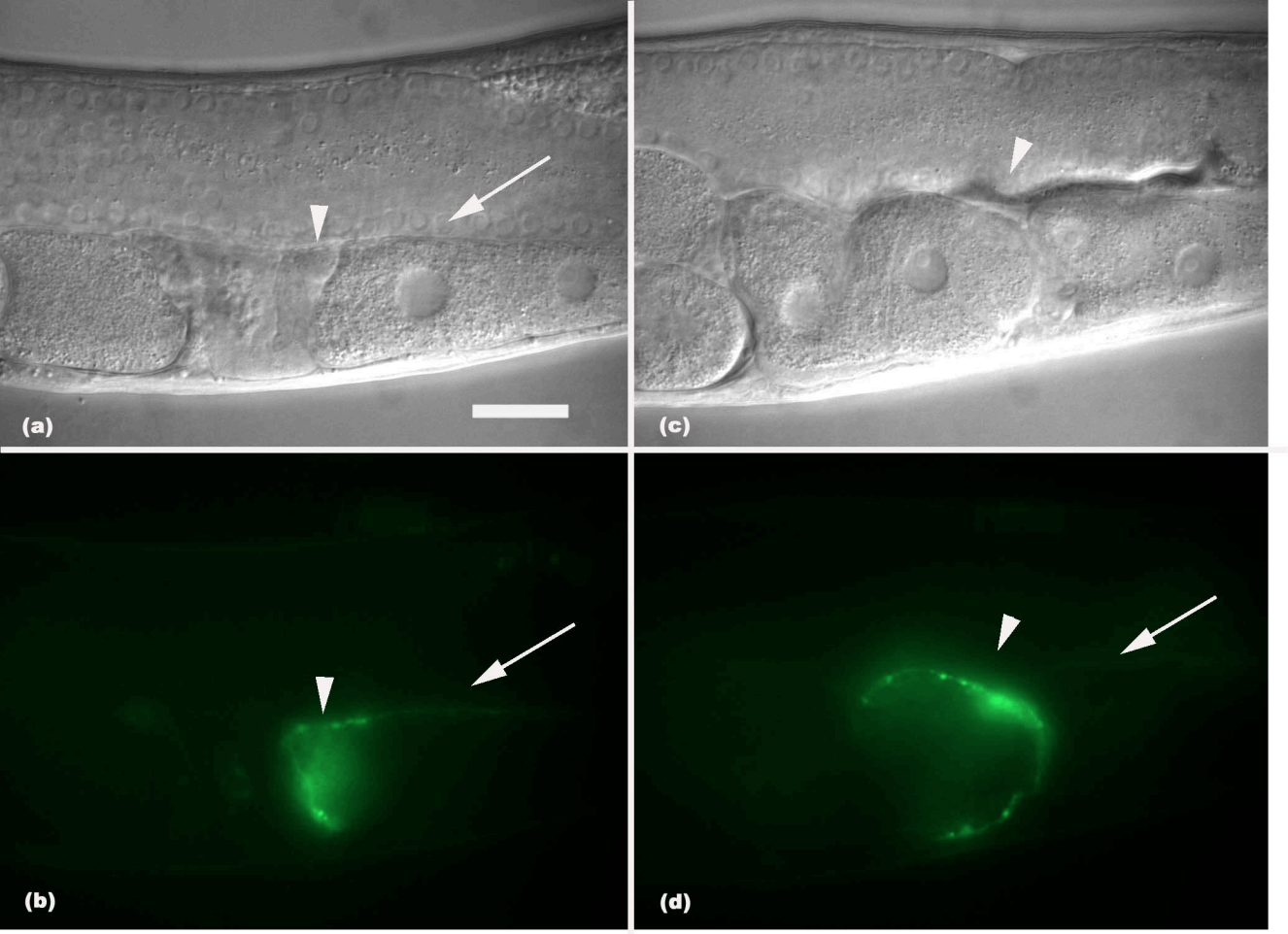
(a)
(c)
(b)
(d)